

SUMMARY OF RECENT AND CURRENT RESEARCH ON ISAR SIGNAL PROCESSING AT THE NATIONAL TECHNICAL UNIVERSITY OF ATHENS, GREECE

Presentation by : Prof. Panayiotis Frangos
'International Technical Laser Workshop
on SLR Tracking of GNSS Constellations'
Metsovo, Greece, 14 – 19 September 2009

1. RECENT RESEARCH

I. 2-D ISAR Signal Modeling and Imaging for Stepped Frequency Modulation

- **main authors** : Anton Lazarov, Professor, Burgas Free University, Anastasios Karakasiliotis, Ph.D. student, NTUA
Panayiotis Frangos, Professor, NTUA.

- **published at** 'IET (IEE) Signal Processing Journal', 2008, Vol. 2, No. 3, pp. 277 – 290, **Special Issue on ISAR Signal Processing Techniques.**

II. Performance analysis of a Parameterized APES (PAPES) method for ISAR Applications

- **main authors** : George Kalognomos and Panayiotis Frangos, School of Electrical and Computer Engineering, NTUA, Greece
- **at late stages of review** in Signal Processing Journal (**August 2009**)

III. Bilinear Time – Frequency Analysis of Radar Signals for ISAR Applications

- **main authors** : George Boultadakis and Panayiotis Frangos, NTUA, Athens, Greece, Lampros Stergioulas, Brunel University, United Kingdom
- **published at** ‘**Electronics and Electrical Engineering**’ Journal, Vol. 92, Nr. 4, pp. 87 – 92, **2009**.

I. 2-D ISAR Signal Modeling and Imaging for Stepped Frequency Modulation

Overview & Simulation Results

Anton Lazarov, Professor, Burgas Free University,
Bulgaria

Anastasios Karakasilotis, Ph.D. Student, NTUA

Panayiotis Frangos, Professor, NTUA

NATIONAL TECHNICAL UNIVERSITY OF ATHENS

2-D ISAR Geometry

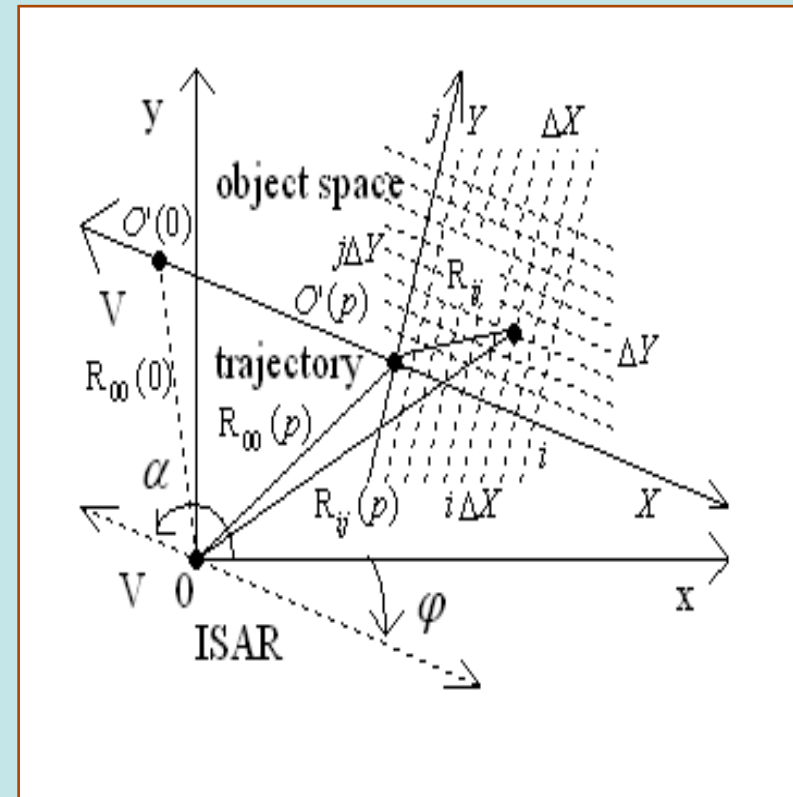
✦ *Level flight of an aircraft, moving along a rectilinear trajectory, at constant speed, without rotational motion (which is the classical approach to the ISAR imaging problem)*

✦ *Target to be imaged is modeled as a rectangular grid of point scatterers, with corresponding scattering intensities describing the geometrical shape of the target*

✦ 2-D geometry:

— *Magnitude of distance vector, $R_{ij}(p)$, from the ISAR to the ij -th point scatterer*

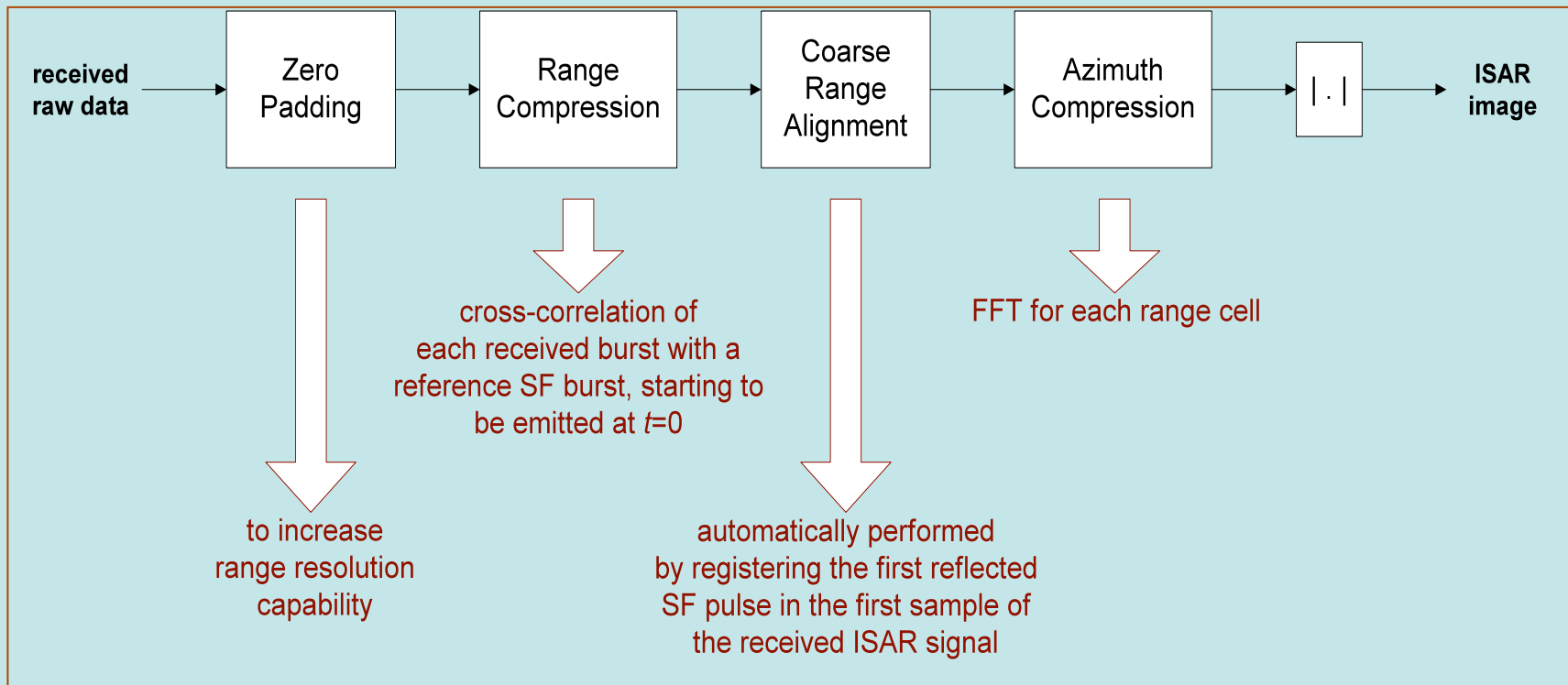
— *Round-trip delay, $t_{ij}(p) = 2 \cdot R_{ij}(p) / c$, of the ISAR signal reflected from the ij -th point scatterer*



2-D SF ISAR Return Signal Model

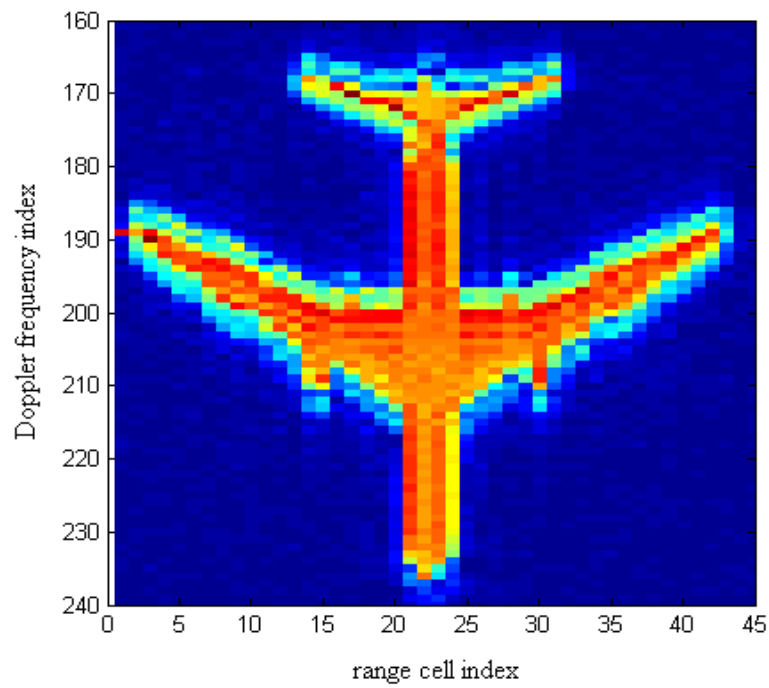
- ✦ *Overall SF ISAR return signal can be considered as the geometrical sum of the individual return signal contributions from the different point scatterers of the target to be imaged*
- ✦ *The process of coherent summation of the backscattered SF modulated pulses has to take into account the round-trip delay, corresponding to each point scatterer, and the frequency of each SF pulse, received at a particular sampling instant.*
- ✦ *White Gaussian noise is added to the SF ISAR return signal.*

2-D SF ISAR Image Reconstruction Process

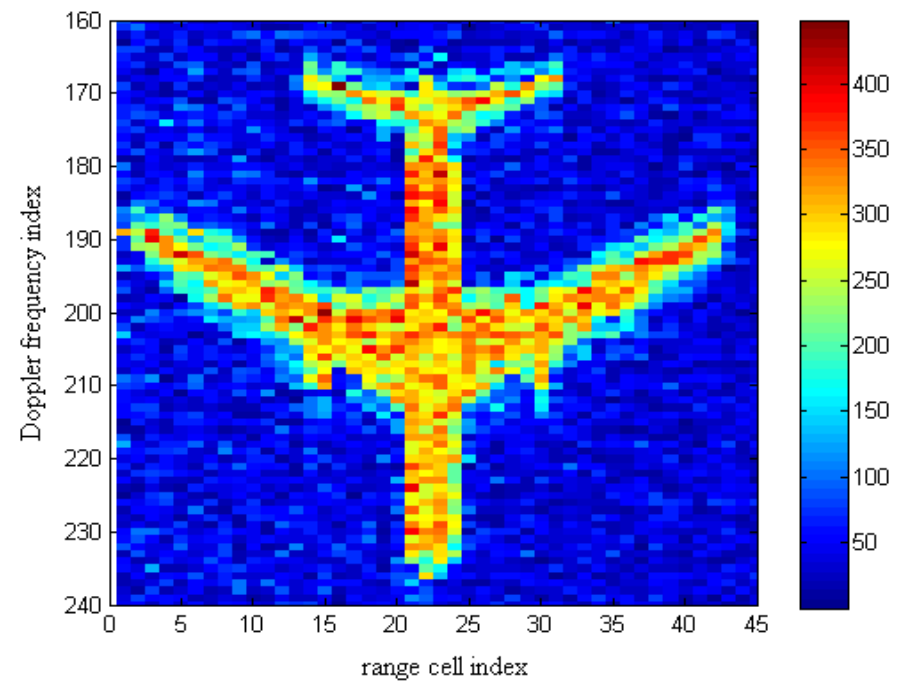


Simulation Results

- ❖ Aircraft geometry of Boeing 737-400 simulated
- ❖ Constant scattering intensity (CSI) values for all point scatterers of the target
- ❖ Signal-to-Noise Ratio (SNR) varied: (a) $SNR = 20\text{dB}$, (b) $SNR = 0\text{dB}$



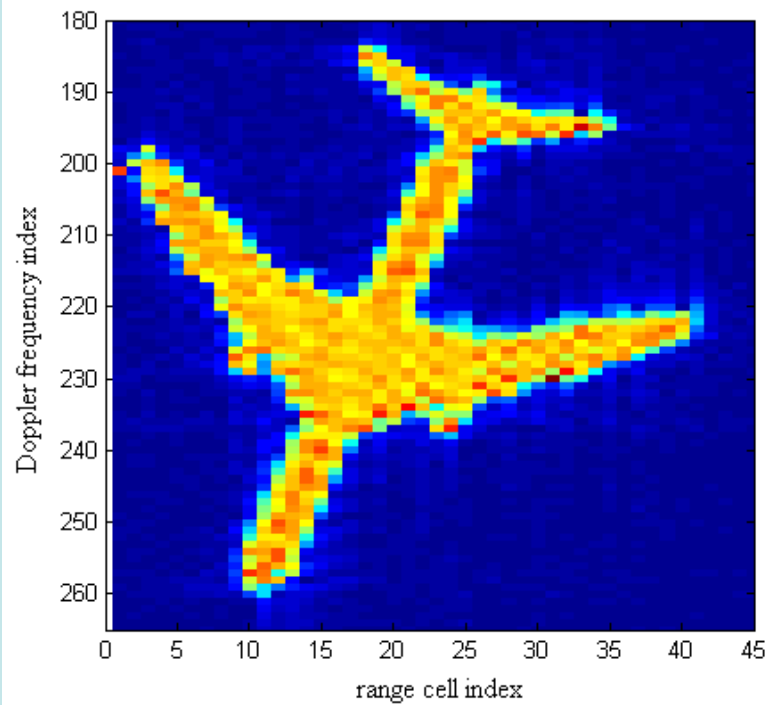
(a)



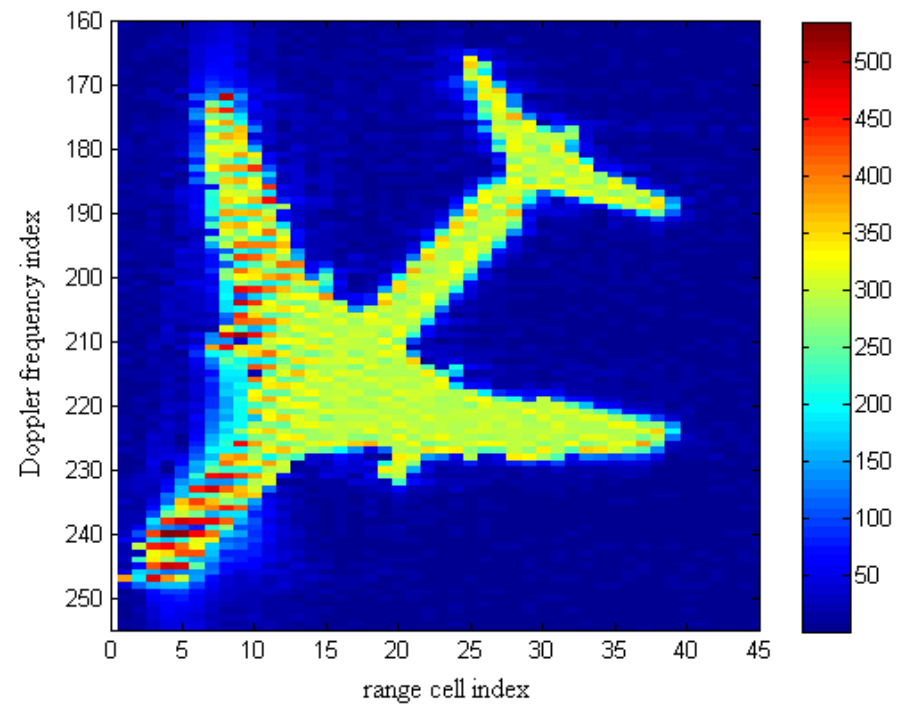
(b)

Simulation Results

- ❖ Aircraft geometry of Boeing 737-400 simulated
- ❖ CSI values for all point scatterers of the target
- ❖ Relatively high SNR value: $SNR = 20\text{dB}$
- Target orientation angle (φ) varied: (a) $\varphi = 20^\circ$, (b) $\varphi = 40^\circ$



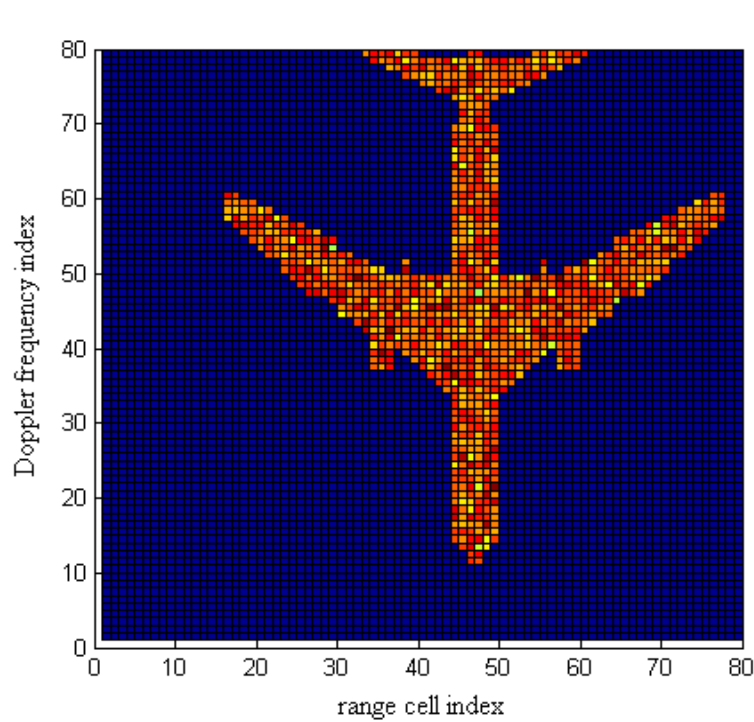
(a)



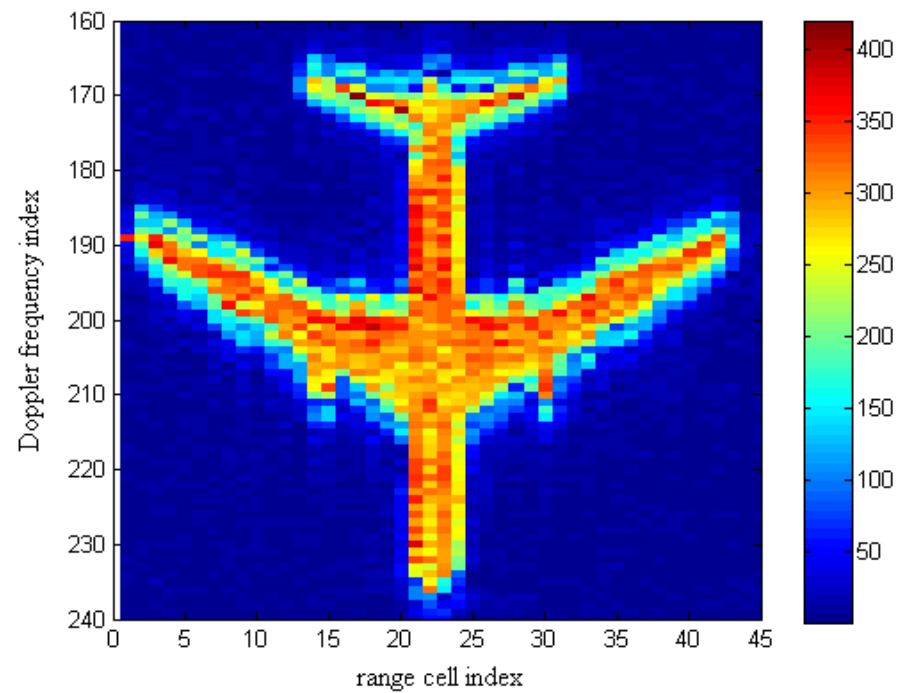
(b)

Simulation Results

- ❖ Aircraft geometry of Boeing 737-400 simulated
 - ❖ Variable scattering intensity (VSI) values for all point scatterers of the target
 - ❖ $SNR = 20\text{dB}$, and, $\varphi = 0^\circ$
- (a) Simulated VSI model, and, (b) reconstructed ISAR image



(a)



(b)

Simulation Results

Calculated entropy values of power normalized ISAR images
and corresponding scattering intensity models

Simulation scenario Aircraft Type		SNR = 20dB			SNR = 0dB	Reference entropy of scattering intensity model
		$\varphi = 0^\circ$	$\varphi = 20^\circ$	$\varphi = 40^\circ$	$\varphi = 0^\circ$	
B-2 stealth		6.0312	6.2817	6.3705	8.0983	6.0684
Mirage 2000C		5.4278	-	-	7.7216	5.3375
Boeing 737-400	CSI	6.9392	7.2061	7.2480	8.6333	6.9236
	VSI	6.8709	-	-	-	6.9060

Conclusions

- ❖ **2-D ISAR images of the simulated targets are well reconstructed through the proposed SF ISAR return signal modeling and imaging approach.**
- ❖ **Even for SNR as low as 0dB, the different aircraft types can be easily recognized from the corresponding ISAR images.**
- ❖ **As target orientation angle becomes greater, the ISAR image entropy increases and some image quality degradation is observed.**
- ❖ **Targets with large wingspan (i.e. B737-400) are more likely to produce unfocused ISAR images, due to a change of the nearest point scatterer during the coherent processing interval.**
- ❖ **VSI model of B737-400 is satisfactorily reconstructed.**
- ❖ **Calculated entropy values for the obtained ISAR images quantify the relative deviation from the corresponding scattering intensity models.**

II. Performance analysis of a Parameterized APES (PAPES) method for ISAR Applications

George Kalognomos, Ph.D. student
Panayiotis Frangos, Professor
School of Electrical and Computer Engineering
National Technical University of Athens
Greece

Spectral estimation problem

- Spectral estimation of a complex 2-D discrete-time signal x_{n_1, n_2} , where $n_1=0, 1, \dots, N_1 - 1$ and $n_2=0, 1, \dots, N_2 - 1$.
- Modeling of $\{x_{n_1, n_2}\}$, using the filterbank approach, for any frequency pair of interest (ω_1, ω_2) :

$$x(n_1, n_2) = a(\omega_1, \omega_2) e^{j(\omega_1 n_1 + \omega_2 n_2)} + w_{n_1, n_2}(\omega_1, \omega_2)$$

- Problem is reduced to that of the estimation of the complex amplitude $a(\omega_1, \omega_2)$ of the 2-D discrete-time data $x(n_1, n_2)$ for all the frequency pairs of interest.

2-D APES method

- Solution of this problem has been investigated in [10] by passing the data of the x_{n_1, n_2} signal through a band pass filter, with varying center frequency. The 2-D APES method gives :

$$\hat{a}_{\text{FB-APES}}(\omega_1, \omega_2) = \frac{\mathbf{b}_{M_1, M_2}^H(\omega_1, \omega_2) \hat{\mathbf{Q}}_{\text{FB-APES}}^{-1}(\omega_1, \omega_2) \bar{\mathbf{Y}}(\omega_1, \omega_2)}{L_1 L_2 \mathbf{b}_{M_1, M_2}^H(\omega_1, \omega_2) \hat{\mathbf{Q}}_{\text{FB-APES}}^{-1}(\omega_1, \omega_2) \mathbf{b}_{M_1, M_2}(\omega_1, \omega_2)}$$

- $\hat{\mathbf{Q}}_{\text{FB-APES}}(\omega_1, \omega_2)$ is the estimation of the noise covariance matrix and it is equal to :

$$\hat{\mathbf{Q}}_{\text{FB-APES}}(\omega_1, \omega_2) = \hat{\mathbf{R}} - \frac{1}{L_1 L_2} \left[\bar{\mathbf{Y}}(\omega_1, \omega_2) \bar{\mathbf{Y}}^H(\omega_1, \omega_2) + \hat{\mathbf{Y}}(\omega_1, \omega_2) \hat{\mathbf{Y}}^H(\omega_1, \omega_2) \right]$$

2-D PAPES method

- Parameterization of $\hat{\mathbf{Q}}_{\text{FB-APES}}(\omega_1, \omega_2)$ with 2 parameters (k_1, k_2) gives :

$$\hat{\mathbf{Q}}_{\text{PAPES}}(\omega_1, \omega_2) = \hat{\mathbf{R}} - \frac{1}{L_1 L_2} [k_1 \bar{\mathbf{Y}}(\omega_1, \omega_2) \bar{\mathbf{Y}}^H(\omega_1, \omega_2) + k_2 \hat{\mathbf{Y}}(\omega_1, \omega_2) \hat{\mathbf{Y}}^H(\omega_1, \omega_2)]$$

- Accordingly the 2-D PAPES method gives

$$\hat{a}_{\text{PAPES}}(\omega_1, \omega_2) = \frac{\mathbf{b}_{M_1, M_2}^H(\omega_1, \omega_2) \hat{\mathbf{Q}}_{\text{PAPES}}^{-1}(\omega_1, \omega_2) \bar{\mathbf{Y}}(\omega_1, \omega_2)}{L_1 L_2 \mathbf{b}_{M_1, M_2}^H(\omega_1, \omega_2) \hat{\mathbf{Q}}_{\text{PAPES}}^{-1}(\omega_1, \omega_2) \mathbf{b}_{M_1, M_2}(\omega_1, \omega_2)}$$

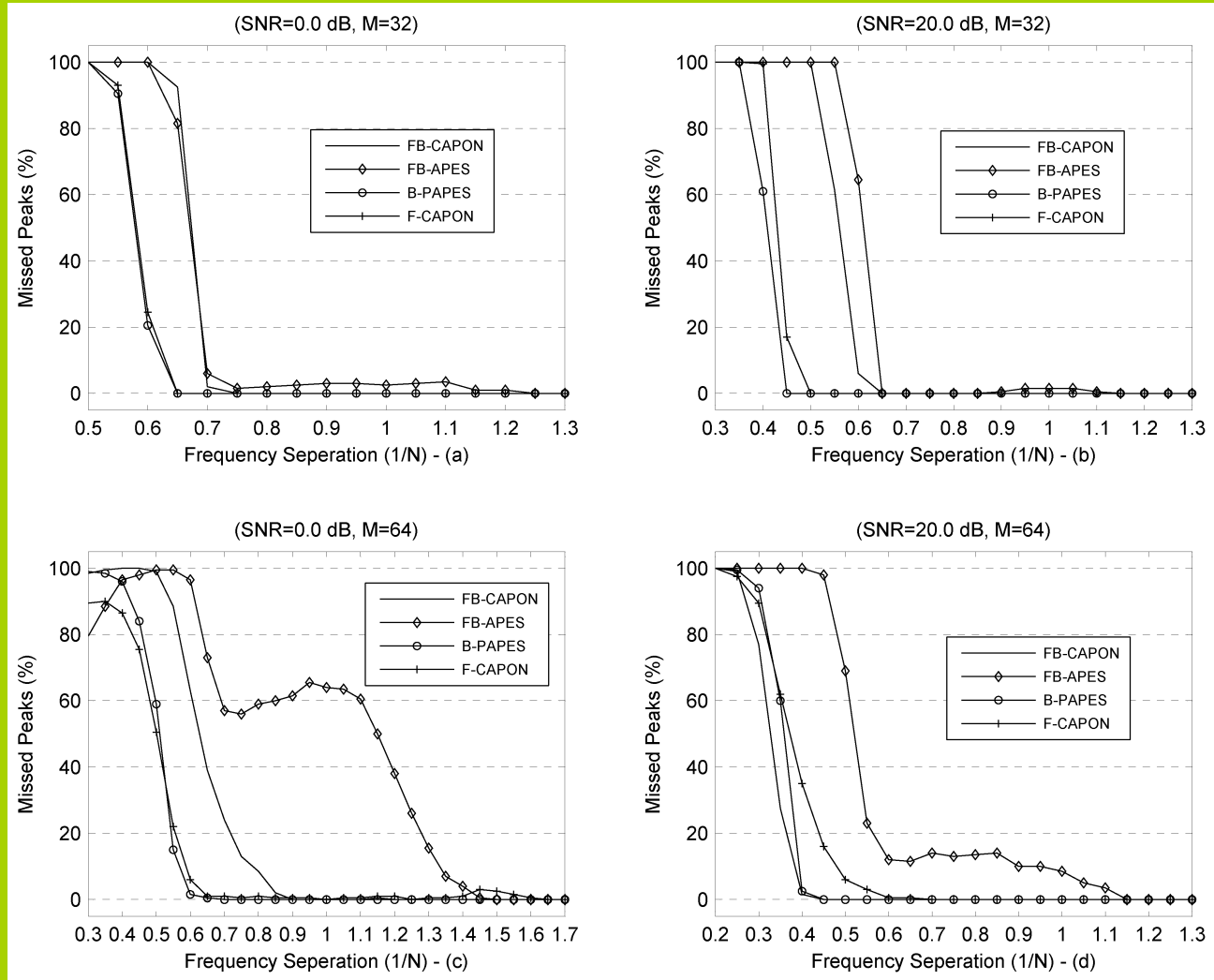
The 2-D PAPES method reduces to 2-D FB-APES method for $(k_1, k_2) = (1, 1)$ and to 2-D FB-CAPON method for $(k_1, k_2) = (0, 0)$

- The new method is called F-PAPES for $(k_1, k_2) = (1, 0)$ and B-PAPES for $(k_1, k_2) = (0, 1)$.

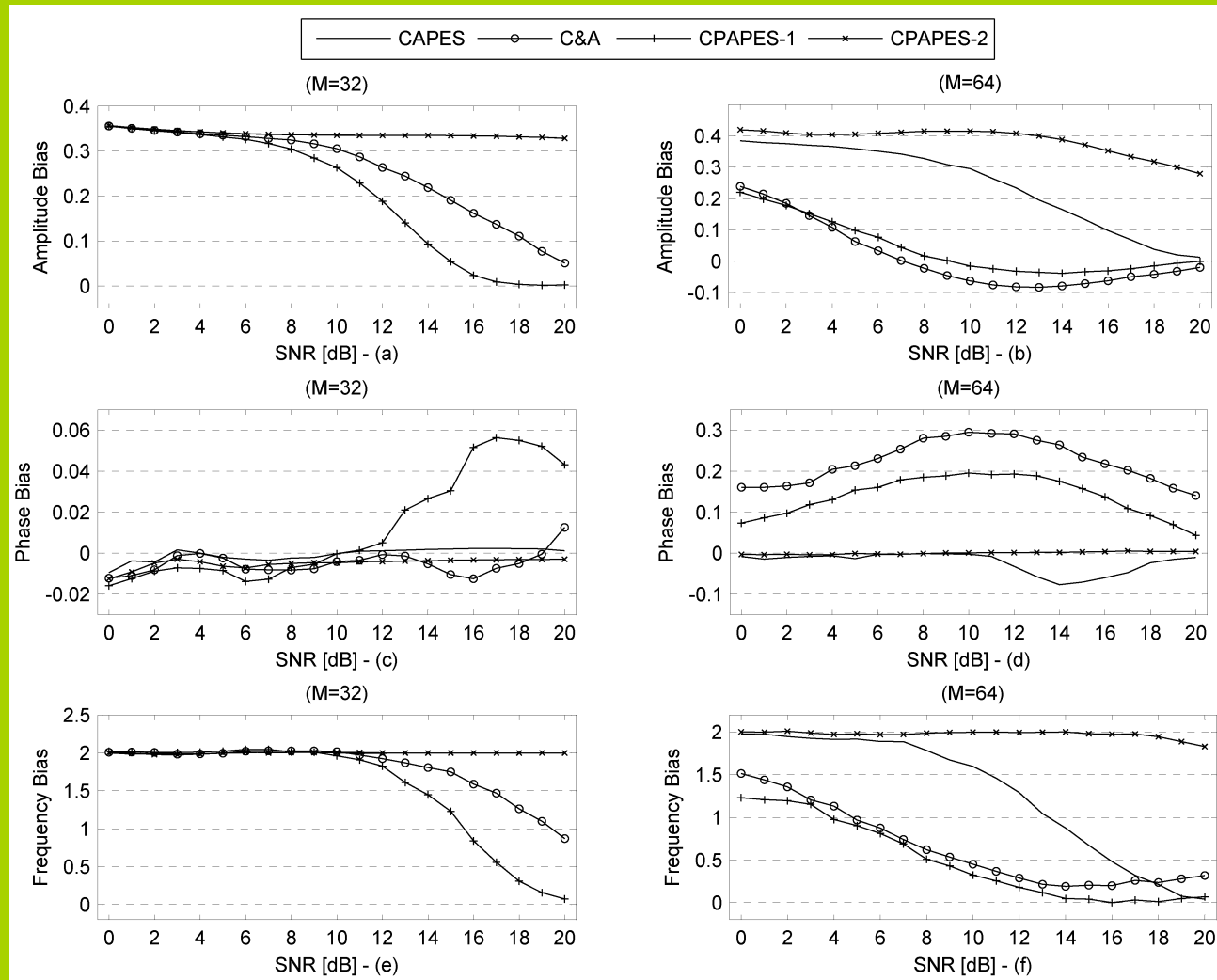
Estimation of spectral lines (SL)

- Combination of CAPON and APES methods by the means of the C&A algorithm was introduced in [6] for the purposes of the estimation of SL :
 - a. Estimation of the spectral peak locations using the F-CAPON method.
 - b. Estimation of the complex amplitude of the SL located in the locations calculated in step (a) by using the FB-APES method.
- Proposed CPAPES-1 algorithm for the estimation of the complex amplitude of SL :
 - a. Estimation of the spectral peak locations using the B-PAPES method.
 - b. Estimation of the complex amplitude of the SL located at the points calculated in step (a) by using the FB-APES method.

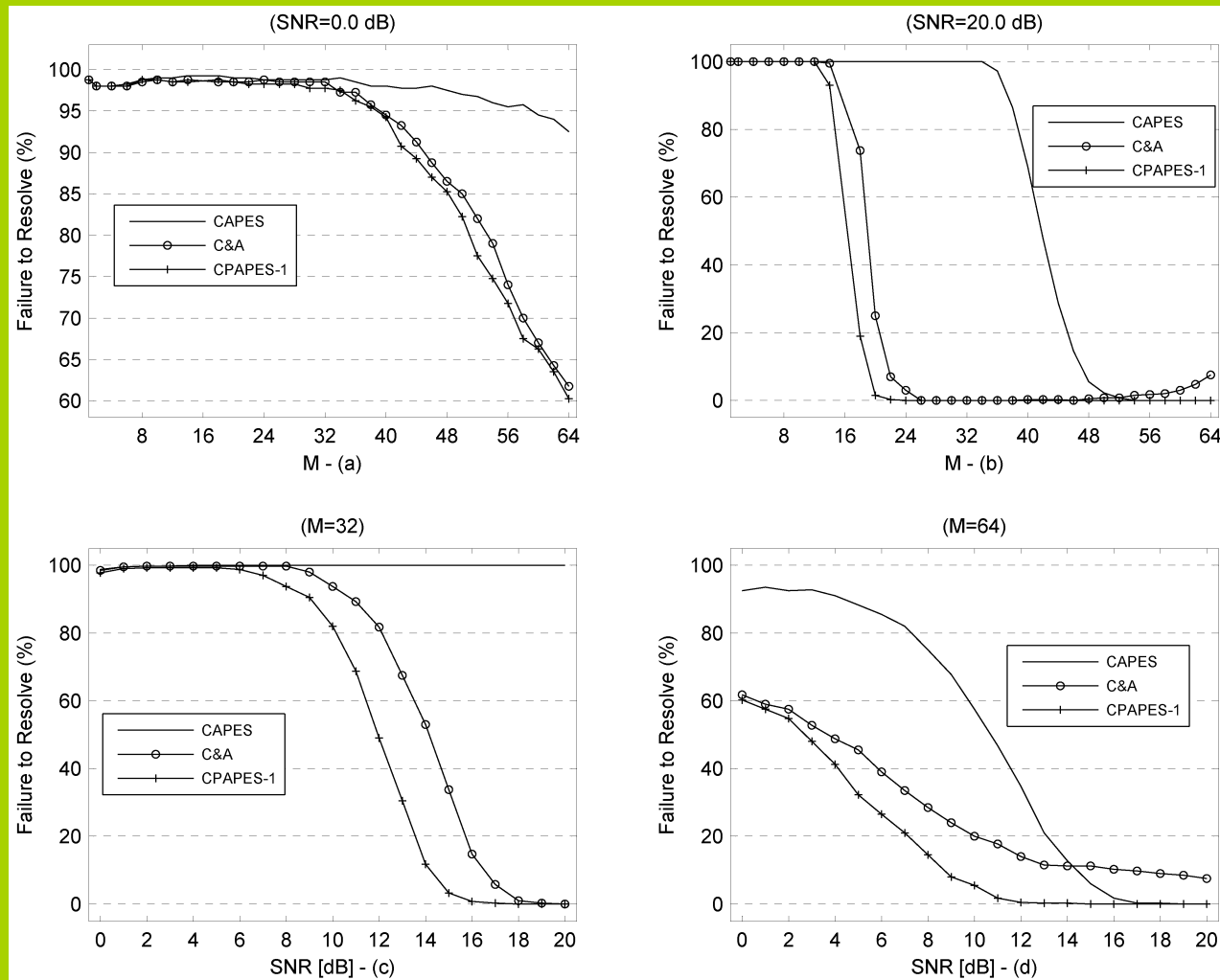
Frequency resolution



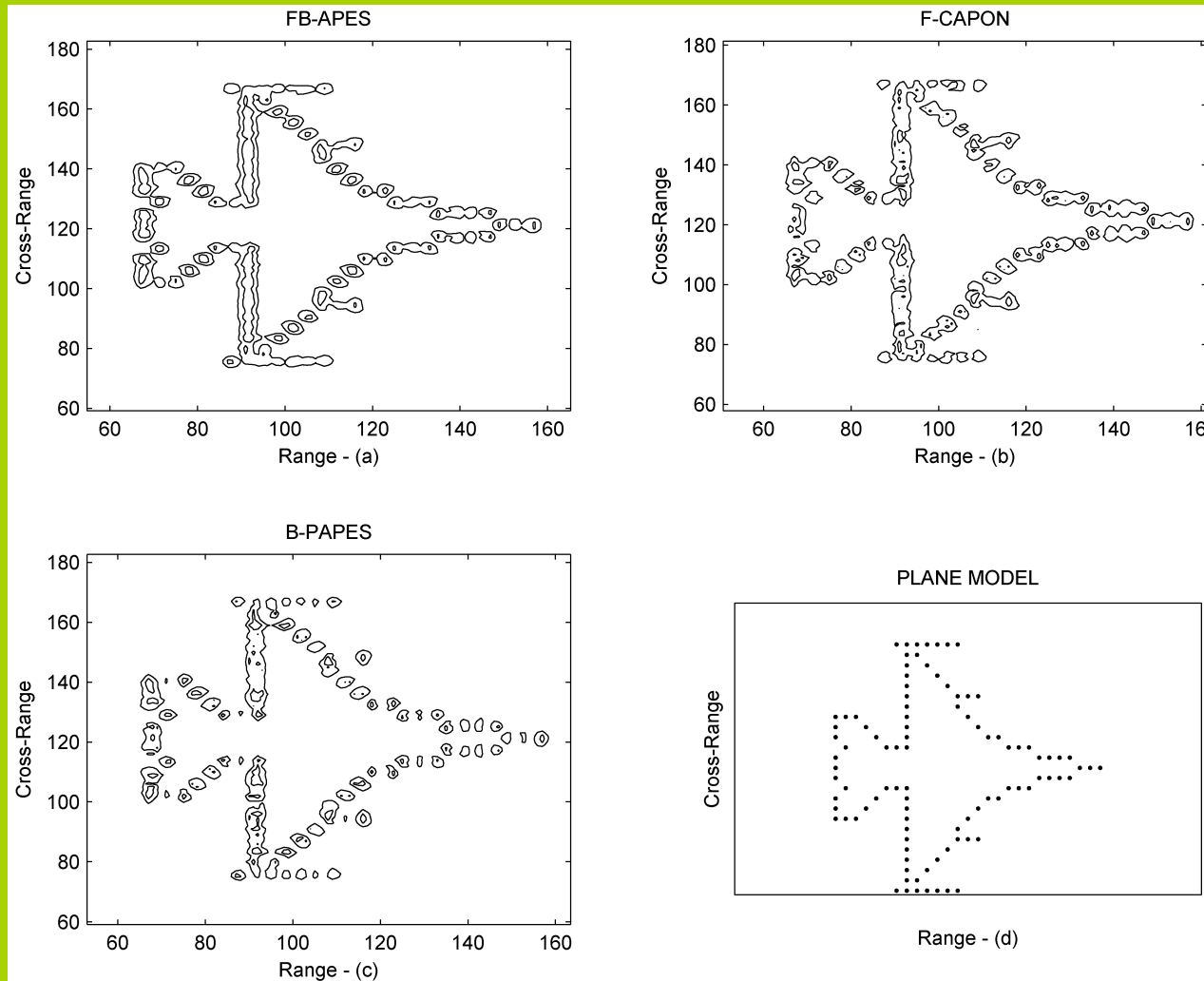
Amplitude/Phase/Frequency Bias



Failure to resolve spectral lines



2-D ISAR Images of a simulated F-16 aircraft for SNR=8 dB



Conclusions

- B-PAPES method is a very suitable candidate for complex spectrum estimation applications where the frequency resolution is of the highest importance since :
 - B-PAPES appears to outperform all the CAPON and APES methods in terms of frequency resolution.
 - B-PAPES appears to outperform the F-CAPON method in terms of amplitude estimation accuracy.
- The combination of the CPAPES-1 and CPAPES-2 algorithms is a very suitable candidate for the complex spectrum estimation of spectral lines.

References

- [1] Stoica P, Moses RL. Spectral analysis of signals. Upper Saddle River, N.J.: Pearson/Prentice Hall 2005.
- [2] Capon J. High-resolution frequency-wavenumber spectrum analysis. Proceedings of the IEEE. 1969;57(8):1408-18.
- [3] Lacoss RT. Data Adaptive Spectral Analysis Methods. Geophysics. 1971;36:661.
- [4] Li J, Stoica P. An adaptive filtering approach to spectral estimation and SAR imaging. Signal Processing, IEEE Transactions on [see also Acoustics, Speech, and Signal Processing, IEEE Transactions on]. 1996;44(6):1469-84.
- [5] Stoica P, Li H, Li J. A new derivation of the APES filter. Signal Processing Letters, IEEE. 1999;6(8):205-6.
- [6] Jakobsson A, Stoica P. Combining Capon and APES for estimation of spectral lines. Circuits, Systems, and Signal Processing. 2000;19(2):159-69.
- [7] Stoica P, Jakobsson A, Li J. Matched-filter bank interpretation of some spectral estimators. Signal Processing. 1998;66(1):45-59.
- [8] Wehner DR. High resolution radar. Norwood, MA: Artech House, Inc. 1987.
- [9] Rihaczek AW, Hershkowitz SJ. Theory and practice of radar target identification, , MA: Artech House, Inc. 2000.
- [10] Li H, Li J, Stoica P. Performance analysis of forward-backward matched-filterbank spectral estimators. Signal Processing, IEEE Transactions on [see also Acoustics, Speech, and Signal Processing, IEEE Transactions on]. 1998;46(7):1954-66.
- [11] Jakobsson A. Model-Based and Matched-Filterbank Signal Analysis. *Ph.D. Thesis*. Uppsala University, Sweden 2000.

‘International Technical Laser Workshop on SLR Tracking of GNSS
Constellations’,
Metsovo, Greece, 14 – 19 September 2009

**“A Comparative Study of Bilinear Time–Frequency
Transforms of ISAR Signals for Air Target
Imaging”**

**G. E. Boultadakis, G. K. Kalognomos, A. V.
Karakasiliotis, P. V. Frangos, L. K. Stergioulas***

Division of Information Transmission Systems and Materials
Technology

School of Electrical and Computer Engineering

National Technical University of Athens

9 Iroon Polytechniou Street, Zografou, GR-15773, Athens, Greece

*Brunel University Uxbridge Middlesex

Bilinear Time-Frequency Transforms

Theoretical background

Incapability of Fourier Transform to analyze “real-life” signals.

Need for Time-Frequency Transform for computing time-varying frequency content of signals and retrieving instantaneous Doppler Frequency information.

The Time-Frequency based image formation uses a transform for each time history series and generates a time-Doppler distribution.

An ISAR image can be obtained for each time instant. Each individual time-sampled ‘frame’ provides image with *superior* resolution.

Our research is to apply Bilinear Time-Frequency Transforms on synthetic radar data and make comparisons on retrieved image quality, in a quantitative manner, using the entropy as a cost function, for several SNR conditions.

Bilinear Time-Frequency Transforms

Theoretical background

Measurement of the degree of image readability, which mainly refers to clarity or “focus” of the image and overall resolution, with a specific image cost function based on entropy.

The value of this cost function is always positive, and the smaller it is, the better the quality of imaging obtained.

The noise is assumed to be Gaussian and white.

For all time-frequency distributions, the *same* window widths (not necessarily the optimal ones), either in time or in frequency, are used for the purpose of a fair comparison of performance.

A 51-point Hamming window is used for time smoothing, whereas a 170-point Hamming window along the time axis is used for the frequency smoothing.

Bilinear Time-Frequency Transforms

Specification of radar/target parameters

Simulated MIG-25 Data was occupied (provided by Dr. Victor Chen).

A MIG-25 is simulated, characterized by 120 point scatterers with equal reflectivity, which are distributed in such a way that the periphery of the aircraft is formed.

The aircraft is simulated in two dimensions.

A radar target can be considered as a collection of finite number of scattering centers, and its scattered signal can be represented as a superposition of the scattered signals from all scattering centers.

Basic motion compensation processing, without polar reformation, has already been applied to the data.

Bilinear Time-Frequency Transforms

Specification of radar/target parameters

The target is assumed to be at a range of 3,500 meters, and its rotation rate to be equal to 10 degrees/sec.

The rotation is assumed about an axis perpendicular to the ISAR plane, which is defined by the radar line of sight (i.e. the line connecting the radar with the target) and the target's linear velocity vector.

Stepped Frequency Radar operating at 9 GHz (X band) with a total bandwidth of 512 MHz. (range resolution equal to 0.29m)

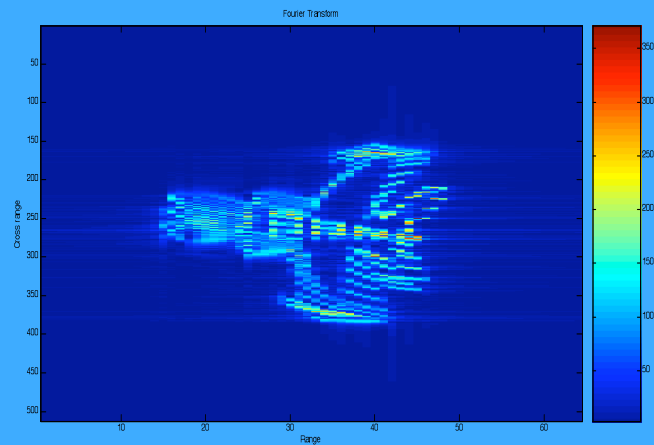
The file contains 512 successive pulses of 64 complex range samples.

'Frame' 256 out of 512 is shown in every Time-Frequency Transform presentation.

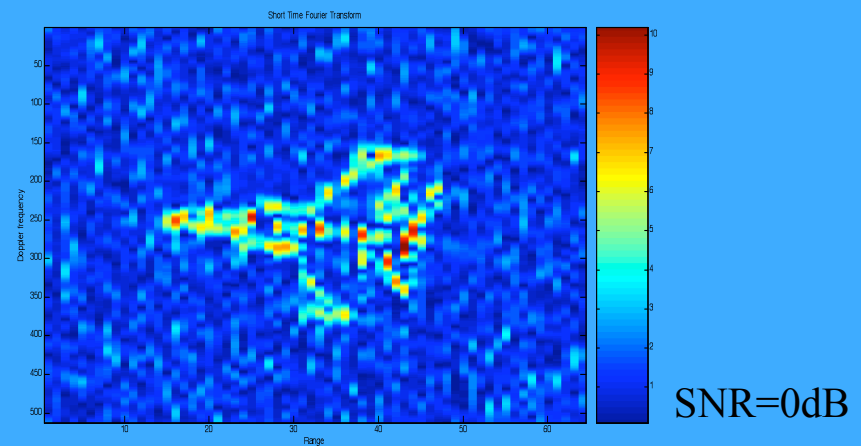
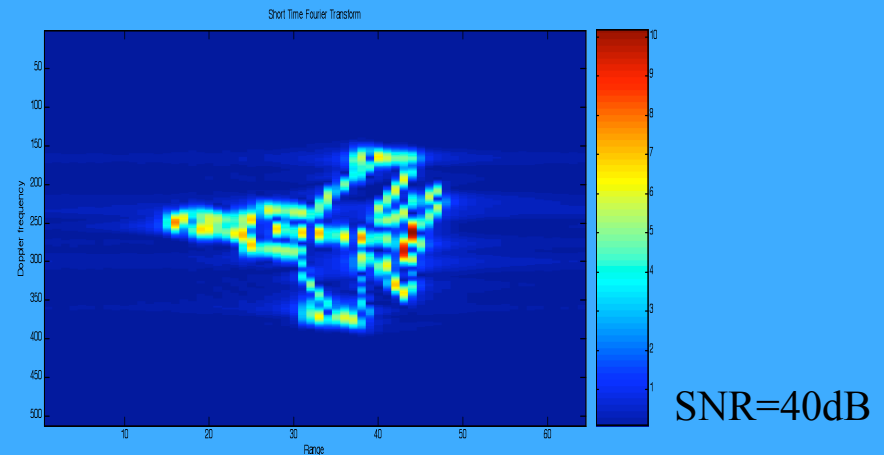
Bilinear Time-Frequency Transforms

Simulation results

2-D Fourier Transform



Short time Fourier Transform

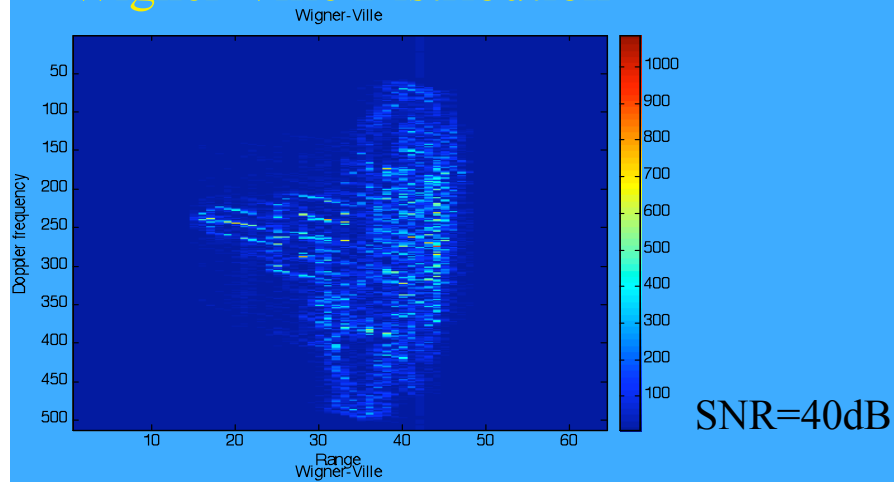


Inadequate results that lead to the use of Bilinear Time-Frequency Transforms

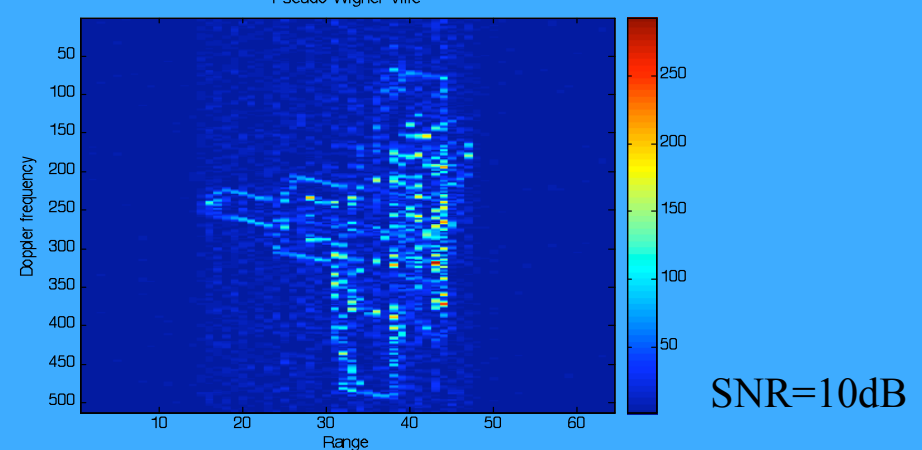
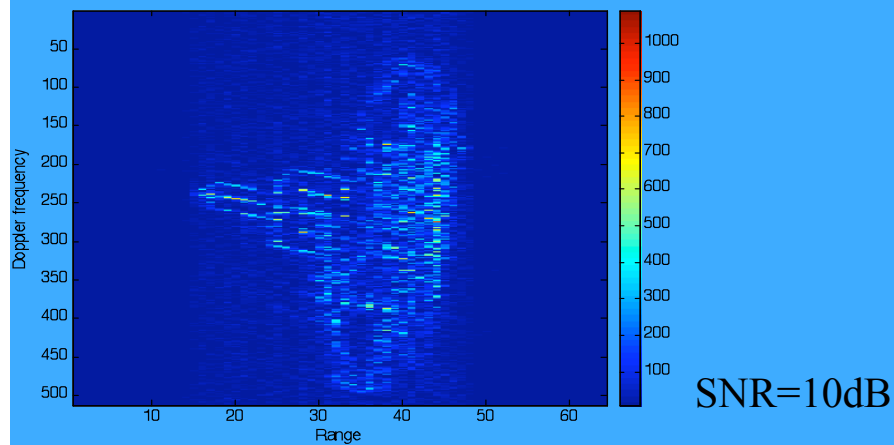
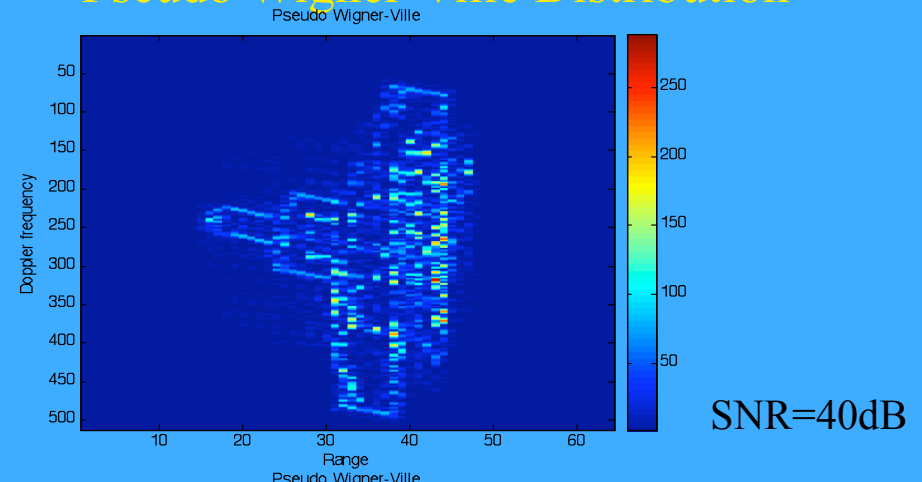
Bilinear Time-Frequency Transforms

Simulation results

Wigner-Ville Distribution



Pseudo Wigner-Ville Distribution

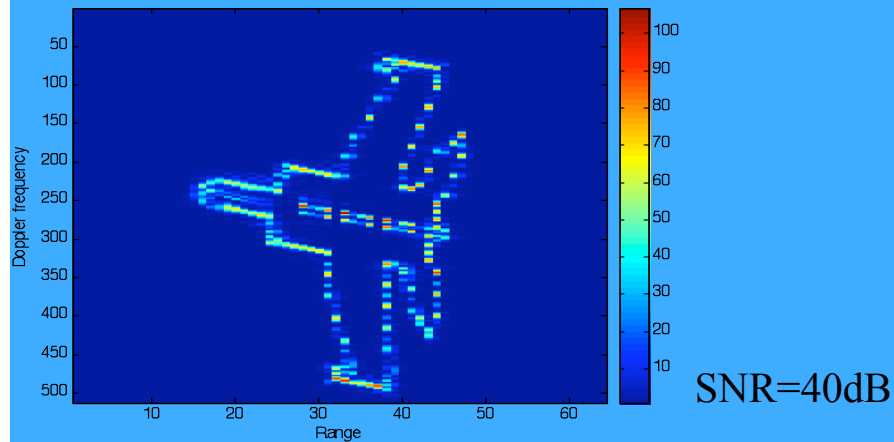


Bilinear Time-Frequency Transforms

Simulation results

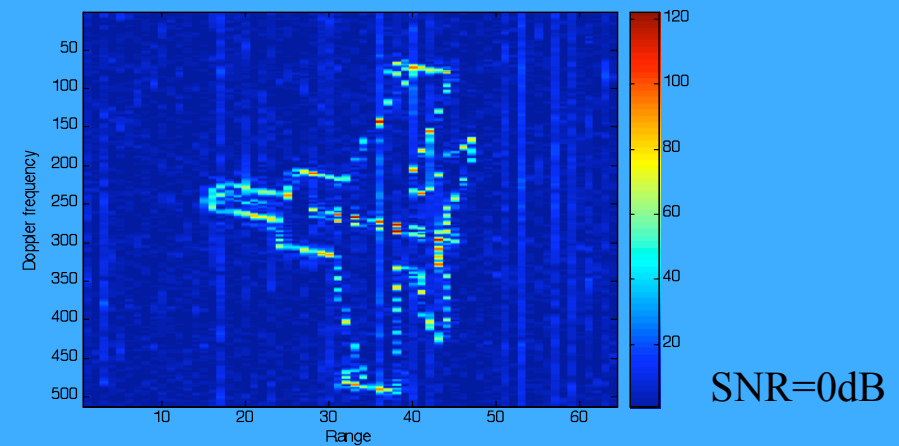
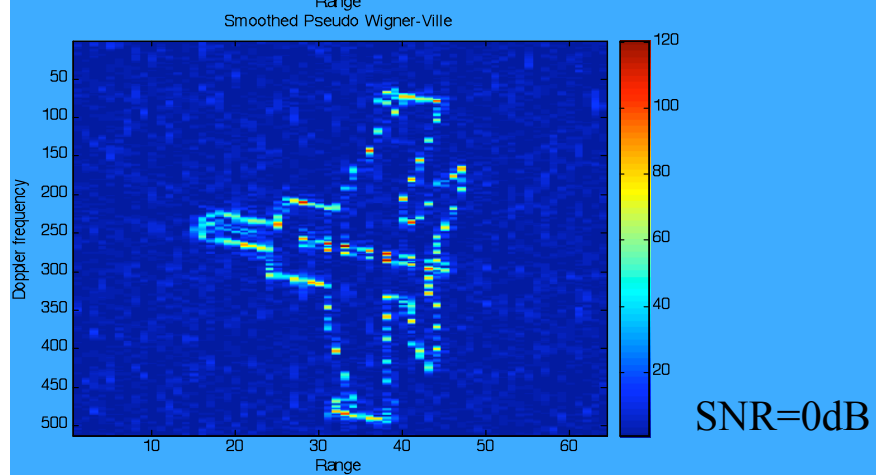
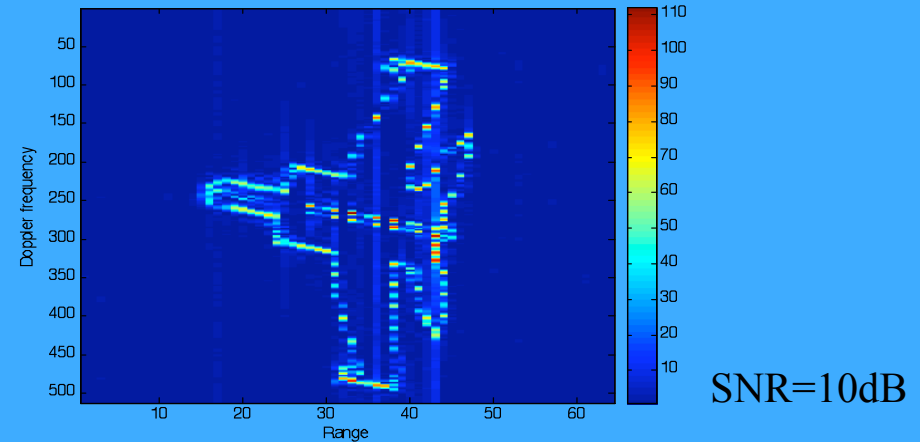
Smoothed Pseudo Wigner-Ville Distribution

Smoothed Pseudo Wigner-Ville



Choi Williams Distribution

Choi Williams



Bilinear Time-Frequency Transforms

Simulation results

Entropy cost function results indicating ISAR imaging performance

	0 dB	10 dB	20 dB	40 dB
Wigner -Ville	8.9665	7.8941	7.6822	7.6540
Pseudo Wigner - Ville	9.0204	7.8593	7.6054	7.5659
Smoothed Pseudo Wigner - Ville	7.6751	7.0670	7.0322	7.0280
Born Jordan	8.2313	7.3924	7.3219	7.3151
Choi Williams	8.1135	7.3288	7.2935	7.2951
Butterworth	8.1416	7.3442	7.3039	7.3045
STFT	9.4918	8.3482	7.9234	7.8502
RID	8.4711	7.5936	7.4944	7.4780
Bessel	8.4241	7.5635	7.4666	7.4501
Zhao Atlas Marks	7.7956	7.3109	7.2847	7.2809

Computation time (PC Intel Centrino 1.6 GHz, 512 MB RAM)

Distribution	Computation time (in sec)
Wigner -Ville	9
Pseudo Wigner - Ville	9
Smoothed Pseudo Wigner - Ville	142
Born Jordan	142
Choi Williams	142
Butterworth	142
STFT	9
RID	142
Bessel	142
Zhao Atlas Marks	142

Bilinear Time-Frequency Transforms

Conclusions

Bilinear Transforms refocus the blurred image of 2-D FFT, caused by fast rotation, without polar reformation, because the time-varying spectrum is well represented.

The Wigner-Ville Distribution, which although it is theoretically optimal and has the maximum number of desired properties, in practice its applicability is rather limited.

The Smoothed Pseudo Wigner-Ville was found to give excellent accuracy as far as quality of image reconstruction is concerned, whereas the Choi-Williams, the Butterworth, the Zhao-Atlas-Marks and the Born-Jordan distributions also yielded images of rather high quality.

Bilinear Time-Frequency Transforms

Future research directions

More emphasis can be given to the geometry of the target, in order to be more realistic, by using either 3-D CAD models for the aircraft targets, or more detailed scattering center representations of the radar target, in which case the Geometrical Theory of Diffraction (GTD) can be used.

A more complicated target motion can also be examined by our research group in the near future, as well as issues concerning possible ways of reduction of the imaging computation time.

Finally, another avenue to explore could be to investigate the application of powerful, newly proposed, optimized Reduced Interference Distributions which are applicable to a wide range of radar signal types, as well as the recently introduced quartic Nested Distributions.

2. CURRENT RESEARCH ON ISAR IMAGING TECHNIQUES

- 2.1 Development of ***autofocusing*** algorithms, based on ***entropy minimization*** of obtained ISAR images (**for fast maneuvering aircraft targets**, in which case scatterers change their range bins within the Coherence Integration Period, CIP)

- 2.2 Specific methods to be used for ***accelerating the implementation of the PAPES method (non – parametric spectrum estimation method)*** introduced in Section 1.11 above, and ***further exploitation of this super-resolution method for the ISAR problem.***